JOURNAL OF GEOPHYSICAL RESEARCH, VOL. 101, NO. A1, PAGES 261–274, JANUARY 1, 1996

Auroral N_2 emissions and the effect of collisional processes on N_2 triplet state vibrational populations

Jeff S. Morrill

E. O. Hulburt Center for Space Research, Naval Research Laboratory, Washington, D. C.

William M. Benesch

Institute for Physical Science and Technology, University of Maryland, College Park

Abstract. Previous model results have shown that the N_2 triplet vibrational level populations in the aurora are strongly affected by cascade and quenching by atomic and molecular oxygen. As the aurora penetrates to lower altitudes (less than 100 km) the role of quenching by atomic oxygen becomes less important and processes involving N_2 collisions begin to play a more prominent part. We are developing a model which will yield steady state vibrational level populations for both the singlet and triplet valence states of N_2. The model currently provides results for the seven low-lying N_2 triplet states ($A\,^3\Sigma_u^+$, $B\,^3\Pi_g$, $W\,^3\Delta_u$, $B'\,^3\Sigma_u^-$, $C^3\Pi_u$, $D^3\Sigma_u^+$, and $E\,^3\Sigma_g^+$). These states are responsible for auroral emissions from the UV (Vegard-Kaplan (VK), second positive (2PG)) through the visible to the infrared (first positive (1PG), infrared afterglow (IRA), Wu-Benesch (WB)). We have included two additional collisional processes in the current model which were not treated previously. These are the intersystem collisional transfer of excitation (ICT) between the *B* state and the *A*, *W*, and *B'* states and vibrational redistribution within the A state vibrational manifold, both due to collisions with ground state N_2. The present work compares our current model results with those of a previous model as well as ground, airborne, and rocket observations. The comparison between $N_2(A)$ (VK) and $N_2(B)$ (1PG) vibrational level populations predicted by our model and a number of auroral observations indicate that the current model achieves a significant improvement in the fit between calculation and observation. In addition, the current model predicts a shift in the band intensity distribution of the 1PG $\Delta v = 3$ sequence from the infrared into the visible red at the lower altitudes (less than 90 km) as well as an overall enhancement in the entire 1PG system. Consequently, this provides a possible explanation of a dominate feature of type *b* aurora, the auroral red lower border.

1. Introduction

The nitrogen molecule, as a major component of the atmosphere, offers great potential as a diagnostic tool to examine energetics and composition in the lower thermosphere. This is largely due to its rich spectrum and the diverse and complex nature of its low-lying excited electronic states. The emission from these excited states in the aurora has long been observed from both the ground and space at wavelengths from the ultraviolet to the infrared. These emissions include the Vegard-Kaplan ($A\,^3\Sigma_u^+ \rightarrow X\,^1\Sigma_g^+$) and second positive ($C\,^3\Pi_u \rightarrow B\,^3\Pi_g$) in the ultraviolet and the first positive ($B\,^3\Pi_g \rightarrow A\,^3\Sigma_u^+$), infrared afterglow ($B'\,^3\Sigma_u^- \leftrightarrow B\,^3\Pi_g$), and Wu-Benesch ($W\,^3\Delta_u \leftrightarrow B\,^3\Pi_g$) in the visible and infrared. In the past the most comprehensive and well-known model of N_2 excited state vibrational level populations was developed by *Cartwright et al.* [1971, 1973] and *Cartwright* [1978]. In the present paper we will focus on a comparison between the results of our current model and those of this previous study.

The early work of *Cartwright et al.* [1971] was motivated in part by the observed altitude variation in the $N_2(A)$ and $N_2(B)$ vibrational distributions inferred from VK and 1PG emission [*Broadfoot and Hunten*, 1964; *Shemansky and Vallance Jones*, 1968]. The work of *Wu and Benesch* [1968] and *Benesch and Saum* [1971] showed the importance of intrasystem cascading between the *W* and *B* states, and *Gilmore* [1969] addressed the potential for similar cascade from the high levels of the *A* state to the lower levels of the *B* state ("reversed" 1PG). The *Cartwright et al.* [1971] model incorporated the intrasystem cascade schemes although the $N_2(B') \leftrightarrow N_2(B)$ transitions were not included until the later model [*Cartwright*, 1978].

The significance of these cascades and other issues (e.g., the amount of 1PG cascade, etc.) was called into question [*Shemansky and Broadfoot*, 1973; *Cartwright et al.*, 1973]. The resulting controversy was resolved in favor of *Cartwright et al.* [1971, 1973] when quantitative measurements of the VK and 1PG by *Vallance Jones* [1974] and *Vallance Jones and Gattinger* [1976a, b, 1978] were compared by *Cartwright* [1978] with his later model results. In addition to questions about cascading there was also disagreement [*Shemansky and Broadfoot*, 1973; *Cartwright et al.*, 1973] on the relative magnitude of the cross sections for electron impact excitation of the low-lying N_2 excited electronic states [*Stanton and St. John*, 1969; *McConkey and Simpson*, 1969; *Brinkmann and Trajmar*, 1970, *Cartwright*, 1970; *Shemansky and Broadfoot*, 1971]. The electron beam studies of *Cartwright et al.* [1977a, b] and *Chutjian et al.* [1977] resolved this controversy in favor of the

Paper number 95JA02835.
0148-0227/96/95JA-02835$05.00

earlier electron beam work of *Brinkmann and Trajmar* [1970]. There have been some improvements to these cross sections [*Ajello and Shemansky*, 1985; *Trajmar et al.*, 1983], but these have not appreciably affected the relative magnitude of the N_2 excited state cross sections. However, there is evidence [*Zubek*, 1994; *Zubek and King*, 1994] that the cross sections for excitation of the $N_2(C)$ state is approximately 20% larger than the values presented by *Trajmar et al.* [1983] and this could impact the interpretation of auroral and airglow 2PG observations.

The N_2 excited state vibrational level population model produced by *Cartwright* [1978] utilized the complex intrasystem cascading scheme, the *Cartwright et al.* [1977b] cross sections, and vibrational level dependent quenching by O, O_2, and N_2. Due to the fit between the above auroral observations and results of *Cartwright's* [1978] model, the N_2 vibrational level populations predicted by that study have remained a point of comparison with auroral observations since that time [*Valance Jones and Gattinger,* 1978; *Torr and Torr*, 1982; *Meier*, 1991].

Cartwright's [1978] model, and other models [*Gattinger and Vallance Jones*, 1979; *Solomon,* 1989; *Strickland et al.*, 1993] which predict vibrational level population of N_2 excited states, focus on radiative cascade and quenching by collisions with O, O_2, and N_2. *Cartwright* [1978] showed conclusively the importance of intrasystem cascade and vibrational level dependent quenching. However, he was forced to rely on both an incomplete set of radiative transition probabilities and less accurate quenching coefficients than are now available. Our current model uses more recent values for both transition probabilities associated with the N_2 triplet transitions [*Gilmore et al.*, 1992; *Piper et al.*, 1989; *Piper,* 1993] and $N_2(A)$ quenching coefficients for collisions with O and O_2 [*Thomas and Kaufman*, 1985]. This model also incorporates two additional collisional processes not previously included in models of atmospheric N_2 emission: the intersystem collisional transfer of excitation (ICT) between vibrational levels of the low-lying N_2 triplet states and vibrational redistribution within the $N_2(A)$ state manifold. The potential for the ICT in low-altitude aurora was addressed by *Cartwright et al.* [1971], *Cartwright* [1978], and *Vallance Jones and Gattinger* [1978], and discussed in detail by *Benesch* [1981, 1983]. As will be shown, by including these collisional processes and updated quenching coefficients and transition probabilities, we have been able to achieve significant improvements in the fit between model results and observations.

Of the two collisional processes the more significant is the intersystem collisional transfer of excitation. This process couples adjacent vibrational levels of overlapping electronic states. For the case of N_2 triplets, this involves the transfer of excitation (excited state population) between vibrational levels of the $B\,^3\Pi_g$ and the $A\,^3\Sigma_u^+$, $W\,^3\Delta_u$, and $B'\,^3\Sigma_u^-$. The potential curves for these states appear in Figure 1, which shows the numerous overlapping vibrational levels which can participate in the ICT processes. We will discuss the details of this process below.

The other collisional process which we include vibrational redistribution within the $N_2(A)$ state, reflects a more appropriate use of the coefficients for $N_2(A)$ quenching by $N_2(X)$ than that of *Cartwright* [1978]. The work on $N_2(A)$ quenching [*Dreyer and Perner*, 1973; *Dreyer et al.* 1974] indicates that collisions between $N_2(A, 2 \le v \le 8)$ and $N_2(X, v = 0)$ lead to a loss of two $N_2(A)$ vibrational quanta with increasing probability as the initial $N_2(A)$ vibrational quantum number increases toward $v = 8$. Dreyer and Perner [1973] and Dreyer et al. [1974] also postulate that this loss of $N_2(A)$ quanta results in the production of an $N_2(X, v = 1)$ molecule. As we will discuss below, we have used the assumption that two (or three) vibrational quanta are lost from the $N_2(A)$ vibrational manifold during this kind of collision while at the same time the electronic energy of the $N_2(A)$ state is retained by the excited molecule.

Including these two additional processes permits a more accurate treatment of the effects of collisions between N_2 ground and excited state molecules. Both of these processes are distinctly different from electronic quenching in that the electronic energy is not lost during the course of the collision. Under these kinds of collisions, either the excited molecule undergoes a transition to an adjacent vibrational level of an overlapping electronic state (ICT) or there is a loss of some number of excited state vibrational quanta (two or three) into a single ground state vibrational quantum. Here we present the preliminary results from our current model and compare them to both *Cartwright's* [1978] model and a number of ground, airborne, and rocket observations.

2. Details of the Vibrational Level Populations Model

2.1. Model Processes

The following processes are included in the current model. The first three processes are generally understood and we will not focus on them in detail. These are the processes which were treated by *Cartwright* [1978].

(1) Electron impact

$$N_2(X) + e^{-*} \rightarrow e^- + N_2(\gamma), \quad \gamma \equiv A, B, W, B', C, D, E$$

and $e^{-*} \equiv$ an energetic electron.

(2) Radiative cascade and intrasystem cascading

$$N_2(\gamma_1) \rightarrow N_2(\gamma_2) + h\nu$$

(3) Electronic quenching

$$N_2(\gamma) + M \rightarrow N_2(X) + M, \quad M \equiv O, O_2, N_2$$

where we do not consider the end products in the quenching reaction, only that the electronic energy of state γ is permanently lost to the N_2 triplet manifold. The new processes are the following:

(4) Intersystem collisional transfer (ICT)

$$N_2(B) + N_2(X) \leftrightarrow N_2(A, W, B') + N_2(X)$$

(5) Vibrational redistribution

$$N_2(A, v_1 \ge 2, 3) + N_2(X, v = 0) \leftrightarrow N_2(A, v_2) + N_2(X, v = 1)$$

with $v_2 = v_1 - 2, 3$

As to the first three processes, the following comments apply. For the current study we use the electron impact excitation rates calculated by *Cartwright* [1978] for altitudes between 100 and 130 km. These rates are a function of the flux and energy distribution of the auroral electrons as well as the energy-dependent cross sections for these excited electronic states [*Cartwright et al.,* 1977b]. The secondary electron spectrum used by *Cartwright* [1978] is based on the measured spectrum

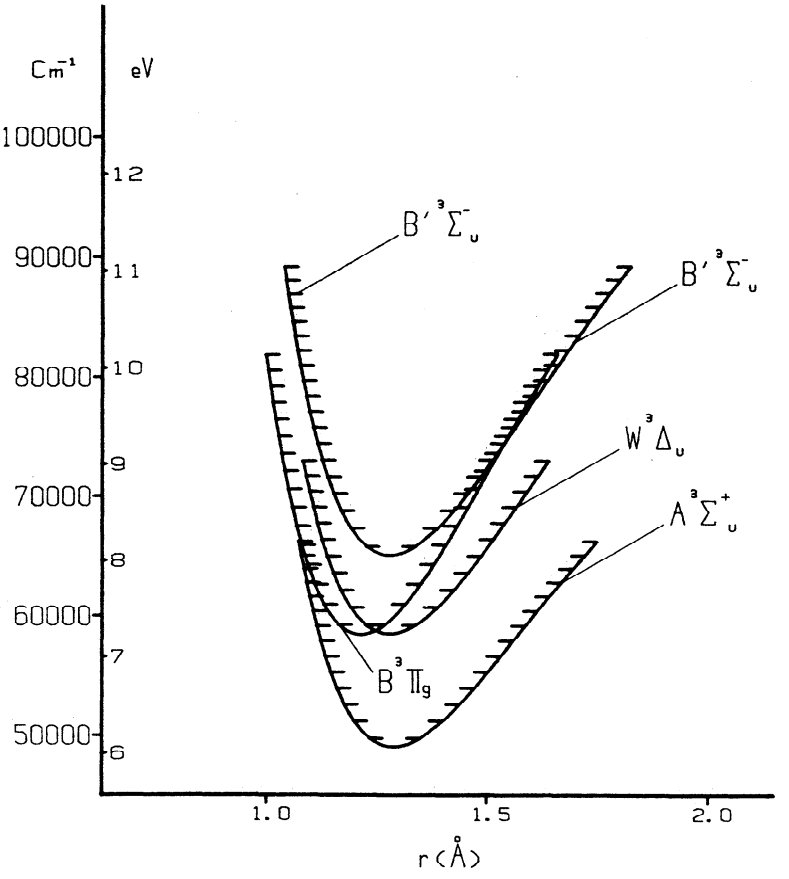

Figure 1. The most significant process which has been included in the current model is the intersystem collisional transfer of excitation (ICT) between the $B\,^3\Pi_g$ and the $A\,^3\Sigma_u^+$, $W\,^3\Delta_u$, and $B'\,^3\Sigma_u^-$. This figure shows the potential curves for the four triplet states which are involved in the ICT process.

of *Feldman and Doering* [1975] for 8 to 100 eV and was extended to higher energies by use of the results of *Rees and Maeda* [1973]. The shape of the spectrum was held fixed but was decreased in magnitude at lower altitudes in a manner consistent with *Feldman and Doering* [1975]. The cascade scheme is the same as with *Cartwright* [1978] (see Table 1) except that we use the more recent transition probabilities of *Gilmore, et al.* [1992], *Piper* [1993], and *Piper et al.* [1989]. For the *D*-to-*E* transition we have used the calculated values for $v' = 0$ from Cartwright's original model (D. C. Cartwright, private communication, 1990).

The scheme for quenching by O, O_2, and N_2 is the same as that of *Cartwright* [1978] except for the $N_2(A)$ state where we use the coefficients for the quenching of $N_2(A)$ by $N_2(X)$ as vibrational redistribution coefficients. We also use the coefficients for quenching by O and O_2 from the work of *Thomas and Kaufman* [1985] combined with the earlier work on O_2 done by *Dreyer et al.* [1974]. Thomas and Kaufman's values and the vibrational redistribution coefficients from *Dreyer et al.* [1974] appear in Figure 2, and the coefficients for quenching of the other excited states by N_2 appears in Figure 3 [*Dreyer and Perner*, 1972; *Cartwright*, 1978]. Quenching of the *D* and *E* states was taken to be identical with that of the *B* state. The vibrational-level-dependent rate coefficients for quenching of $N_2(A)$ by O and O_2 were used for all seven triplet excited states, as with *Cartwright* [1978].

The stability of N_2 excited states with regard to O and O_2 quenching was discussed by *Cartwright* [1978]. At that time coefficients for quenching by these species had been measured only for $N_2(A)$. Based on stability arguments, Cartwright chose to use the quenching coefficients of $N_2(A)$ by O and O_2 for all excited states. Since that time a number of measurements of quenching coefficients for N_2 singlets ($a^1\Pi_g$ and $a'^1\Sigma_u^-$) by O_2

Table 1. Cascade Scheme

Transition	Common Name
Normal Cascade	
$A\,^3\Sigma_u^+ \rightarrow X\,^1\Sigma_g^+$	Vegard-Kaplan
$C\,^3\Pi_u \rightarrow B\,^3\Pi_g$	Second positive
$D\,^3\Sigma_u^+ \rightarrow B\,^3\Pi_g$	Fourth positive
$D\,^3\Sigma_u^+ \rightarrow E\,^3\Sigma_g^+$	--------
$E\,^3\Sigma_g^+ \rightarrow A\,^3\Sigma_u^+$	Herman-Kaplan
$E\,^3\Sigma_g^+ \rightarrow B\,^3\Pi_g$	--------
$E\,^3\Sigma_g^+ \rightarrow C\,^3\Pi_u$	--------
Intrasystem cascade	
$B\,^3\Pi_g \leftrightarrow A\,^3\Sigma_u^+$	First positive (and reverse)
$B'\,^3\Sigma_u^- \leftrightarrow B\,^3\Pi_g$	Infrared-afterglow
$W\,^3\Delta_u \leftrightarrow B\,^3\Pi_g$	Wu-Benesch

These are the ten transitions used in the current model. See text for discussion

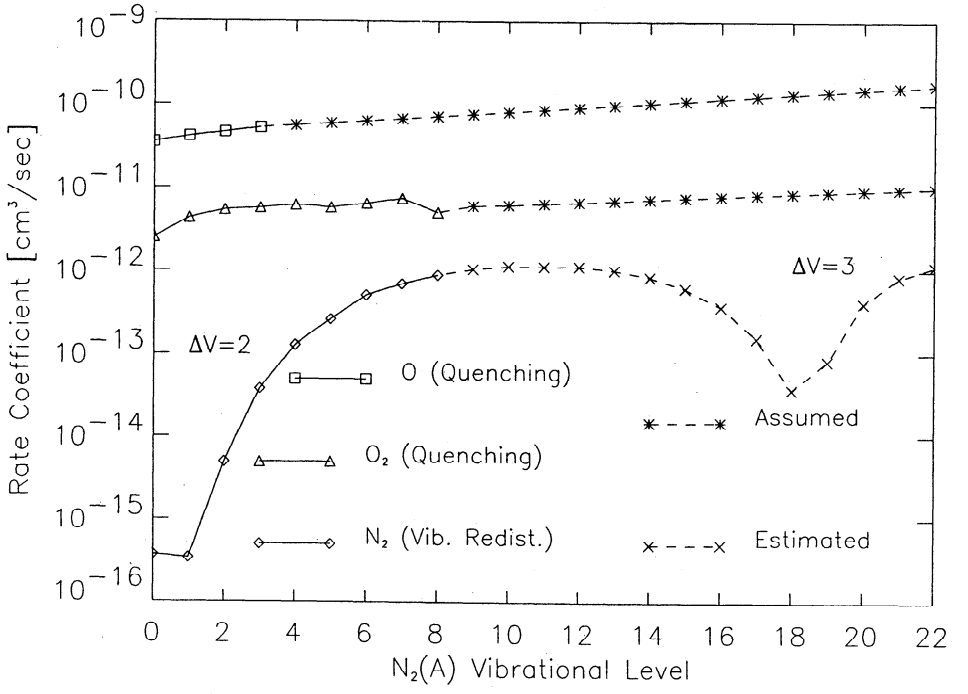

Figure 2. The quenching coefficients for the $A^3\Sigma_u^+$ used in the current model. The points connected by solid curves are measured values and those connected by dashed curves are extrapolated or estimated. Three major differences between the current values and those of *Cartwright* [1978] are (1) a slight increase the O quenching coefficient, (2) an improvement in the O_2 quenching coefficients for $v = 1$ and 3 [*Thomas and Kaufman*, 1985], and (3) the use of the N_2 quenching coefficients for vibrational redistribution within the $A^3\Sigma_u^+$ vibrational manifold [*Dreyer et al.*, 1974].

have been done [*Marinelli et al.*, 1989; *Piper*, 1987]. The results indicate that the quenching coefficients for these two states are larger than originally assumed by *Cartwright* [1978] which carries the implications for similar increases for the triplet excited states. However, since the above studies do not distinguish between electronic quenching and collisional transfer they must be interpreted carefully. Collisional transfer from the $N_2(W)$ and $N_2(A)$ states to the $N_2(B)$ state, induced by collisions with O_2, has been observed by *Bachmann et al.* [1992, 1993]. Given that a focus of the current study is the addition of N_2 collisional processes to previous models and for comparison with the results of *Cartwright* [1978], we have chosen to use Cart-

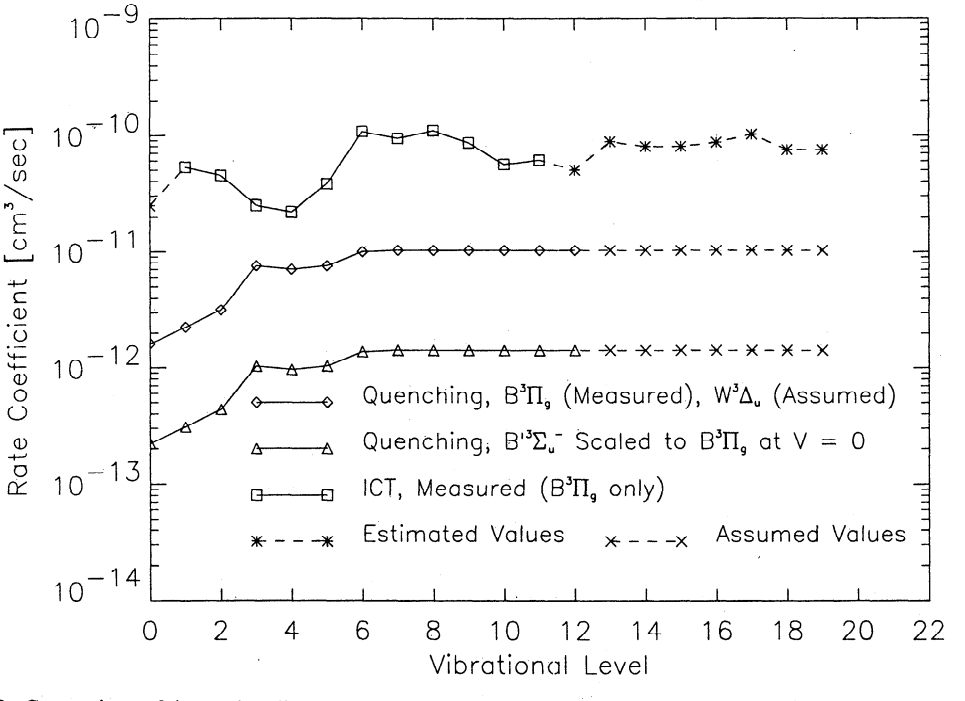

Figure 3. Comparison of the total collisional transfer rates from the $B\,^3\Pi_g$ with the quenching coefficients used by both the current model and *Cartwright's* [1978]. Also shown are the quenching rate coefficients for $W\,^3\Delta_u$ and $B'\,^3\Sigma_u^-$.

wright's quenching scheme. Since we are mostly concerned with the effects at lower thermospheric altitudes where N_2 is the dominant species and the resulting intersystem collisional transfer rates are quite large, the impact of the uncertainties in the O and O_2 quenching coefficients will be small. This could effect the interpretation of observations at higher altitudes where atomic oxygen is the dominate collision partner and so warrants further examination.

2.2. Intersystem Collisional Transfer of Excitation

The ICT process couples vibrational level populations of overlapping electronic states and should not be considered a simple quenching process. The name is based on the fact that collisions transfer excitation (or population and thereby emission intensity) from one emission system (WB) to another (1PG). This process has been examined in numerous laboratory studies [*Heidner et al.*, 1976; *Sadeghi and Setser*, 1981; *Rotem and Rosenwaks*, 1983; *Benesch and Fraedrich*, 1984; *Katayama*, 1984; *Ali and Dagdigian* 1987; *Morrill et al.*, 1988; *Bachmann, et al.*, 1992, 1993 and references contained therein] but it has only recently been included in models of atmospheric emission [*Morrill and Benesch*, 1994, 1995; *Eastes et al.*, 1994].

Rate coefficients for this process have been measured [*Rotem and Rosenwaks*, 1983; *Espy*, 1986; *Katayama and Dentamaro*, 1989; *Bachmann et al.*, 1992, 1993; J. S. Morrill and W. M. Benesch, manuscript in progress] and the theoretical aspects of these transitions have also been examined [*Alexander and Pouilly*, 1983; *Alexander and Corey*, 1986; *Ali and Dagdigian*, 1987]. For the current model, the rate coefficients for collisional transfer between the $N_2(B)$ state and the $N_2(A)$, $N_2(W)$, and $N_2(B')$ states are based on the measured values of *Rotem and Rosenwaks* [1983]. We consider these rate coefficients to reflect the sum of rate coefficients for collisional transfer from the $N_2(B)$ state to the $N_2(A)$, $N_2(W)$, and $N_2(B')$ states. These coefficients are shown in Figure 3. In order to partition these rate coefficients from a given $N_2(B)$ level to a set of nearby levels of the $N_2(A)$, $N_2(W)$, and $N_2(B')$ states, we have assumed (1) that only transfers to the nearest vibrational levels of the overlapping $N_2(A)$, $N_2(W)$, and $N_2(B')$ states are important and (2) that the rates scale as $(g_\gamma/g_B)\exp|\Delta E|$. In the latter approximation, ΔE is the energy difference between the two vibrational levels involved in the transition and g_γ/g_B is the ratio of the degeneracies of the two states. The exponential term in the above approximation is used to weight more heavily, transitions between levels which have nearly the same energy. The return values from these three states to the $N_2(B)$ were based on the formulation by *Benesch and Fraedrich* [1984] such that,

$$k_{WB}/k_{BW} = (Q_W/Q_B)(g_W/g_B) \sim (B_B/B_W)(g_W/g_B),$$

where the Qs are the rotational partition functions, the g's are the electronic state degeneracies, and the Bs are the rotational constants for the specific states and levels in question. We have used the simple model presented by *Bachmann et al.* [1992, 1993] to estimate rate coefficients for levels which have no measured values (B,$v = 0$ and $v \geq 12$, see Table 2).

The use of estimated rate coefficients does involve some uncertainty since the role of rotational energy levels in determining resonance between adjacent vibrational levels or the importance (or lack of importance) of the Franck-Condon factor between a given pair of adjacent levels is not yet completely understood. Nonetheless, these recent values and current empirical estimates are of adequate quality to allow the inclusion of this process in our current model. However, the details of collisional transfer still require further experimental and theoretical examination.

During the study of the collisional transfer process [*Rotem et al.*, 1982; *Benesch*, 1983; *Alexander and Pouilly*, 1983;

Table 2. Intersystem Collisional Transfer Rate Coefficients

$B^3\Pi_g$		$A\,^3\Sigma_u^+$		$W\,^3\Delta_u$		$B'\,^3\Sigma_u^-$
0	7	7.83	0	17.2		
1	8	6.14	1	41.7		
	9	5.21				
2	10	22.0	2	22.7		
3	11	8.57	3	9.06		
	12	2.78	4	4.59		
4	12	0.95	4	2.33	0	8.49
	13	6.00	5	4.23		
5	14	8.52	6	15.0	1	11.7
	15	2.69				
6	15	3.68	7	58.0	2	18.3
	16	28.1				
7	17	11.1	8	59.9	3	13.1
	18	9.75				
8	19	35.3	9	43.4	4	14.1
	20	6.97	10	6.77	5	3.52
9	20	4.41	10	6.46	5	8.72
	21	36.9	11	10.2	6	3.58
	22	4.18				
10	22	3.93	11	6.46	6	4.62
	23	21.9	12	6.46	7	2.99
	24	3.24				
11	24	3.20	12	3.25	7	3.47
	25	18.9	13	22.5	8	3.43
	26	5.67				
	27	1.31				
12	26	5.67	14	28.2	8	2.08
	27	5.30			9	3.78
	28	13.3				
13			15	62.4	9	2.35
			16	19.2	10	4.54
14			16	45.5	10	2.11
			17	27.2	11	5.34
15			17	33.5	11	1.93
			18	38.4	12	6.14
16			18	24.9	12	1.82
			19	53.5	13	6.92
17			19	18.8	13	1.75
			20	73.8	14	7.60
18			21	65.7	14	1.72
					15	8.16

Intersystem collisional transfer rate coefficients from the $N_2(B)$ state to the $N_2(A)$, $N_2(W)$, and $N_2(B')$ states used in the current model. Rate coefficients are in units of 10^{-12} cm^3/molecule-s The left most column is the $N_2(B)$ state vibrational level. The columns of numbers under each other term symbol are the vibrational quantum numbers of the overlapping levels and the rate coefficient from the $N_2(B)$ state. Return rate coefficients are scaled as discussed in the text.

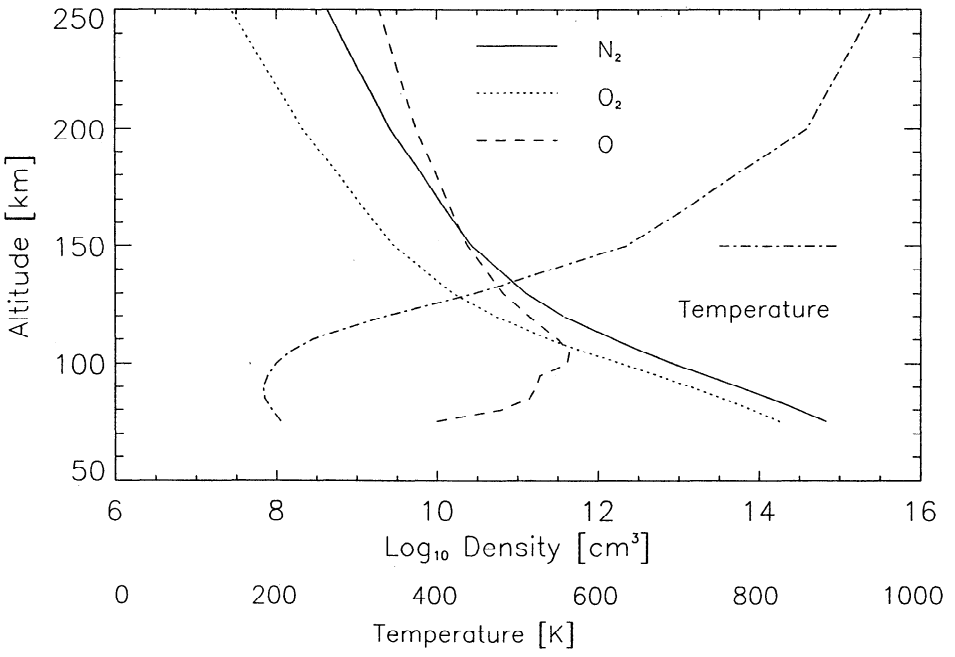

Figure 4. The atmospheric model used for the present results [*Jursa*, 1985] which was used for the density and temperature inputs required by the model. This model atmosphere is similar to that used by *Cartwright* [1978].

Katayama and Dentamaro, 1986; *Ali and Dagdigian*, 1987; *Piper*, 1988; *Bachmann et al.*, 1992, 1993] a number of selection rules have come to light. These selection rules appear to be those for dipole allowed transitions ($\Delta\Lambda = 0, \pm 1$, $\Delta S = 0$, $g \leftrightarrow u$, $g(u) \not\leftrightarrow g(u)$). The consequence of these rules is that ICT transitions within the N_2 triplet manifold occur between the $B\,^3\Pi_g$ and the $A\,^3\Sigma_u^+$, $W\,^3\Delta_u$, and $B'\,^3\Sigma_u^-$ but no transitions occur among the latter three states.

2.3. Vibrational Redistribution within the $N_2(A)$ State

According to *Dreyer and Perner* [1973] and Dreyer et al. [1974] who studied quenching of $N_2(A)$ by $N_2(X)$, the loss of population from $N_2(A,v_1)$ equals the gain in population into $N_2(A,v_2)$ where $v_1 - v_2 = 2$ for $2 \le v_1 \le 7$. They attributed this loss of two $N_2(A)$ vibrational quanta to the production of $N_2(X,v = 1)$ from $N_2(X, v = 0)$. In addition, they note that as the $N_2(A)$

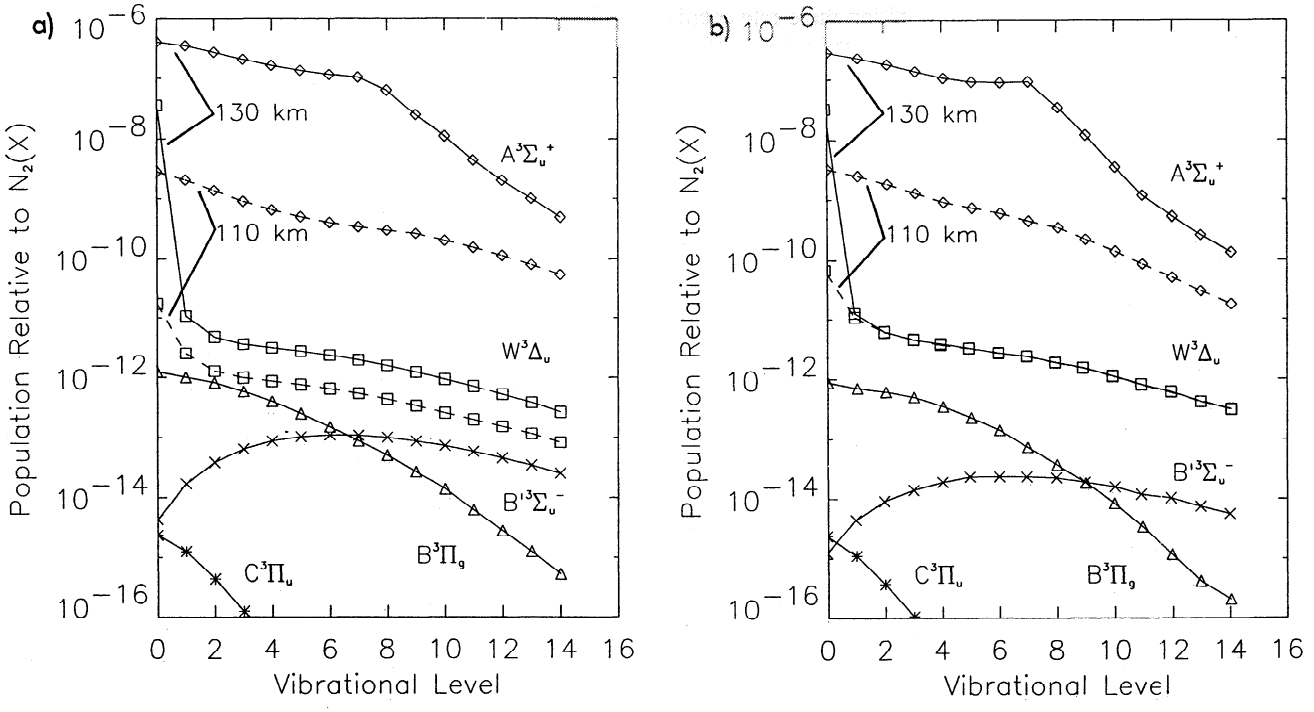

Figure 5. These figures compare results from (a) the current model with (b) those of *Cartwright* [1978] for 130 km (without quenching) and 110 km (with quenching only). The solid and dashed curves for $A\,^3\Sigma_u^+$ and $W\,^3\Delta_u$ are for 130 and 110 km, respectively. Note that the curves for $W\,^3\Delta_u$ at 130 and 110 km overlap in Figure 5b for $v = 2$ and above. The curves for $B\,^3\Pi_g$, $B'\,^3\Sigma_u^-$, and $C\,^3\Pi_u$ are for 130 km without quenching.

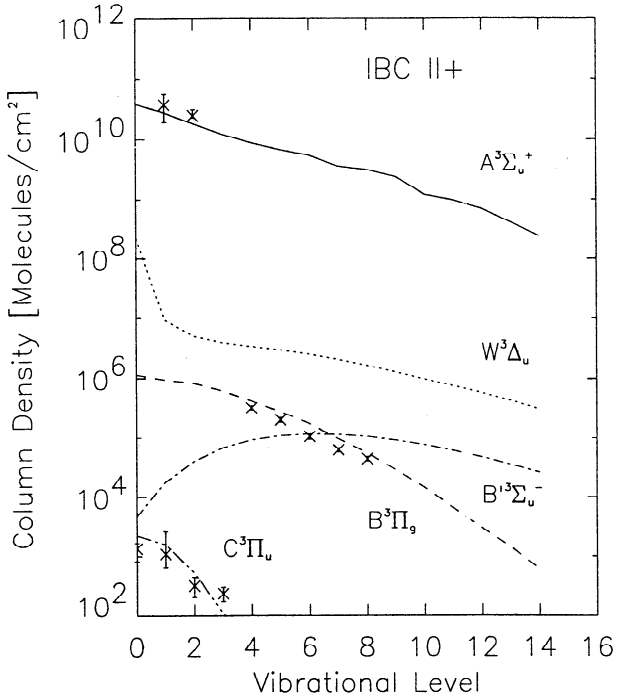

Figure 6. Column abundances predicted by the current model between 100 km and 250 km for the five indicated states. Also shown are the column abundances for $N_2(A)$, $N_2(B)$, and $N_2(C)$ states implied by the observations of Rees et al. [1976] scaled to the current results.

vibrational level increases so does the resonance between $\Delta v = 2$ in the $N_2(A)$ and the energy difference between the two lowest levels of $N_2(X)$. Their data show a corresponding increase in rate coefficient with increasing vibrational level. In order to extrapolate to higher $N_2(A)$ levels we have fit Dreyer and Perner's rate coefficients to a power series in $\exp(-|\Delta E|)$ where

$$\Delta E = [(E_{A,v1} - E_{A,v2}) - (E_{X,v=1} - E_{X,v=0})].$$

Since this function peaks between $v = 8$ and 12 for $\Delta v = 2$ we have used the resulting polynomial to estimate rate coefficients for higher $N_2(A)$ vibrational levels ($v \geq 16$) using $\Delta v = 3$ in the $N_2(A)$ state. The results appear in Figure 2. An important point to note is that *Cartwright's* [1978] use of the values for the quenching of $N_2(A)$ by $N_2(X)$ reduces the total $N_2(A)$ population. Conversely, our use of the values in Figure 2 does not affect the total $N_2(A)$ population but rather forces the vibrational distribution toward the lower levels.

2.4. Equations for Statistical Equilibrium

In order to determine the equilibrium vibrational level populations of the N_2 triplet excited states, we solve the equation for statistical equilibrium below. This is a master equation which is based on the processes mentioned above and is similar to the formulation used by *Cartwright* [1978]. For a given vibrational level v, in a given state α, the equation which describes the relative number density (n_v^α / n_{N2}) at statistical equilibrium is

$$K_{ei;v}^{\alpha} + \sum_\beta \sum_I (A_{i,v}^{\beta\alpha} + K_{ICT;i,v}^{\beta\alpha} + \delta_{A\beta}\,\delta_{i,v+2(3)}\,K_{VR;i,v}^{A})\,(n_i^\beta/n_{N2}) =$$
$$\{K_{q;v}^{\alpha} + \sum_\gamma \sum_j (A_{v,j}^{\alpha\gamma} + K_{ICT;v,j}^{\alpha\gamma} + \delta_{A\gamma}\,\delta_{v,j+2(3)}\,K_{VR;v,j}^{A})\}\,(n_v^\alpha/n_{N2}) \quad (1)$$

where

$K_{ei;v}^{\alpha}$ electron impact excitation rate (per N_2) of vibrational level v in state α;
$A_{i,v}^{\beta\alpha}$ transition probability from $\beta(I)$ to $\alpha(v)$;
$K_{ICT;i,v}^{\beta\alpha}$ intersystem collisional transfer rate from $\beta(I)$ to $\alpha(v)$;
$K_{VR;i,v}^{A}$ vibrational redistribution rate from $A(I)$ to $A(v)$;
$K_{q;v}^{\alpha} = k_{q(O);v}^{\alpha}(n_O) + k_{q(02);v}^{\alpha}(n_{O2}) + k_{q(N2);v}^{\alpha}(n_{N2})$ total quenching rate;
α, β, γ electronic states;
i,j source and sink vibrational levels, respectively.

All rates are in Hertz. $K_{ei;v}^{\alpha}$ also includes enhancements due to elevated ground vibrational distributions [*Morrill and Benesch,* 1990]. The two Kronecker deltas insure the k_{VR} term (vibrational redistribution) applies only to the $N_2(A)$ state and only for $\Delta v = 2$ or 3. An important point about the ICT rates is that for any given $B\,^3\Pi_g$ vibrational level only the nearest (quasi-isoenergetic) vibrational levels of $A\,^3\Sigma_u^+$, $W\,^3\Delta_u$, $B'\,^3\Sigma_u^-$ are involved in the ICT processes and so many of these terms are zero (see Table 2).

Currently, the model requires as inputs volume excitation rates (per N_2) for the seven excited states as well as temperature and density (O, O_2, N_2) from a model atmosphere. In order to present an effective comparison we have used the volume excitation rates from *Cartwright* [1978;Table 1] and the CIRA-72 model atmosphere for intermediate solar conditions and a 1000 K exospheric temperature [Jursa, 1985]. The model atmosphere we have used is shown in Figure 4. Calculations for altitudes above 130 km or below 100 km used the volume excitation rates at these altitudes, respectively, as well as the density and temperature provided by the model atmosphere for the specific altitude in question.

3. Results

The Figures 5a and 5b compare results from the current model with those of *Cartwright* [1978] for 130 km (without quenching) and 110 km (with quenching only). The solid and dashed curves for $A\,^3\Sigma_u^+$ and $W\,^3\Delta_u$ are for 130 and 110 km, respectively. The curves for $B^3\Pi_g$, $B'\,^3\Sigma_u^-$, and $C\,^3\Pi_u$ are for 130 km without quenching. The major difference between the two Figures involves the stronger effect of quenching in the current model on the overall $W\,^3\Delta_u$ populations at 110 km. The current model also predicts an enhancement in the $B\,^3\Pi_g$ and $B'\,^3\Sigma_u^-$ overall populations compared to the model of *Cartwright* [1978].

A rigorous test of any model of N_2 populations in the aurora involves its ability to predict the column abundances of the N_2 triplet state molecules. Calculated densities summed from 100 to 250 km are shown in Figure 6. Also shown are the abundances implied by the results of *Rees et al.* [1976] scaled to fit the predicted $N_2(A)$, $N_2(B)$, and $N_2(C)$ state distributions. The excitation rates used for the model results are for an IBC II+ aurora (5577 Å > 10 kR) whereas the observation of Rees et al [1976] were made when the 5577 Å emission ranged from 5 to 7 kR. The fit between observation and model results is very good with the observations of *Rees et al.* [1976] being scaled up by a factor of 8.5. It should be noted that any effects of collisional processes at lower altitude are not expected to be seen in this type of observation due to the dominant role of the emission from the peak in the emission profile (approximately 110 km).

Figure 7 compares calculated $A^3\Sigma_u^+$ populations from our current model with *Cartwright's* [1978] model. Also shown are

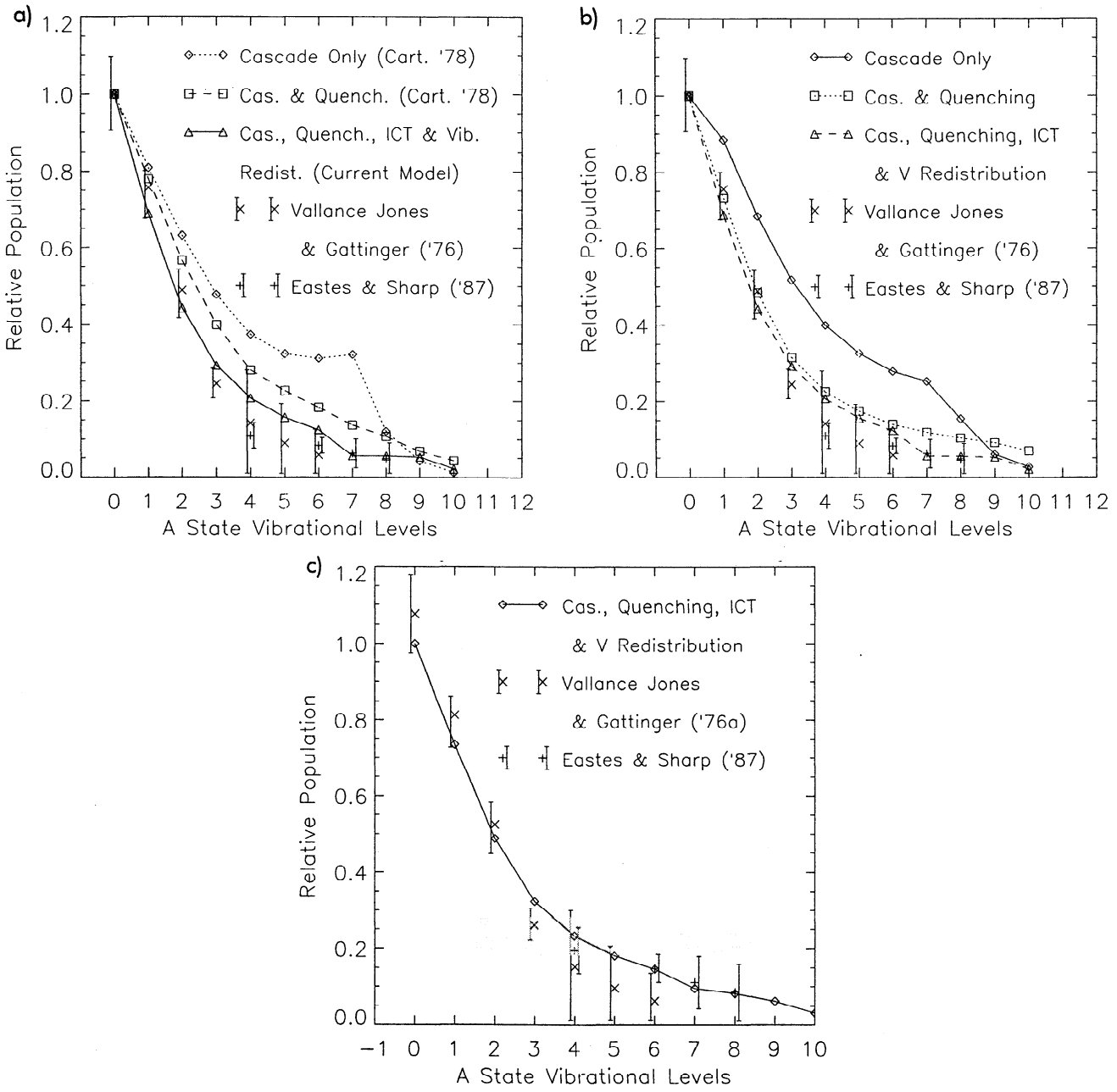

Figure 7. These three figures compare model $A\,^3\Sigma_u^+$ populations from our current model and *Cartwright's* [1978] with the observations of *Vallance Jones and Gattinger* [1976a] and *Eastes and Sharp* [1987]. Figure 7a compares *Cartwright's* [1978] results (with and without quenching) with the current model results with quenching, ICT, and vibrational redistribution all active. Figure 7b shows results from the current model alone and differentiates runs where various collisional processes were active. In Figure 7a and 7b the two data sets have been scaled to overlap at vibrational levels 4 and 6. Figure 7c compares the $A^3\Sigma_u^+$ column density distribution from Figure 5 with the above observations. Here both data sets have been scaled to the model distribution independently.

ground and rocket observations of relative $N_2(A)$ populations from VK emissions [*Vallance Jones and Gattinger*, 1976a ; *Eastes and Sharp*, 1987] (herein after referred to as VJ&G and E&S, respectively) which have been scaled using the recent transition probabilities of *Piper* [1993]. In this figure the model distributions are for 110 km as are the observations of E&S, whereas the VJ&G results are for integrated column emission. Figure 7a compares *Cartwright's* results (with and without quenching) with those of the current model when quenching, ICT, and vibrational redistribution are all active. This figure shows a significant enhancement in the populations of the lower levels predicted by the current model. Figure 7b shows results from the current model alone at 110 km and displays the results of model runs where different collisional processes were active. For the lower vibrational levels, the enhancement of the populations is largely due to the use of improved transition probabilities and quenching coefficients for collisions with O and O_2. Vibrational redistribution appears to have only a slight effect on the relative populations of these levels at this altitude. The effect of ICT can be seen for $v = 7$ and above.

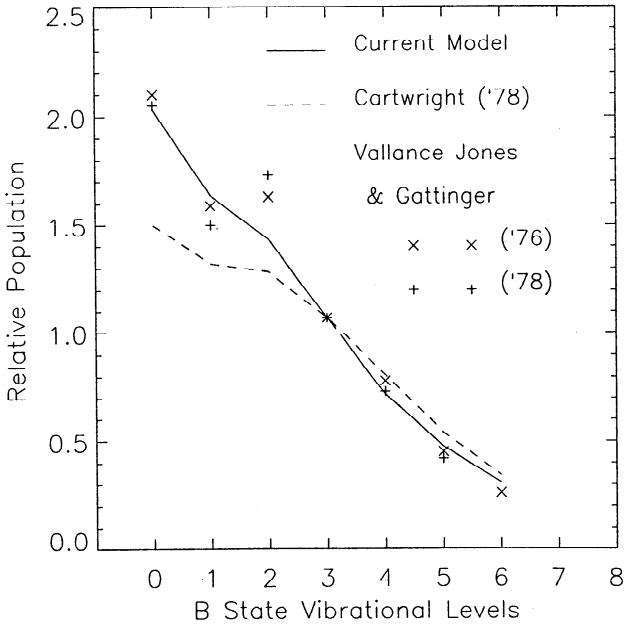

Figure 8. Comparison of $B\ ^3\Pi_g$ populations predicted by the current model at 110 km with all collisional processes active and the model results of *Cartwright* [1978]. Also shown are the observations of *Vallance Jones and Gattinger* [1976, 1978].

The results in Figure 7c compare the $N_2(A)$ predicted vibrational distribution implied by column emission (Figure 6) with the VJ&G and E&S data. This is a more comprehensive comparison of the VJ&G data with model results than is shown by Figures 7a and 7b. In Figure 7c the VJ&G and E&S data is scaled to the model distribution independently unlike the scaling on Figures 7a and 7b where the two distributions are scaled together at $v = 4$ and 6 and the $v = 0$ populaton is set to unity. The independent scaling is reasonable for Figure 7c since the E&S data fits equally well the relative distribution for $v = 4$-8 derived from either column densities measurements or emission spectra from a specific altitude.

Figure 8 compares $B\ ^3\Pi_g$ populations predicted by the current model at 110 km, using all three collisional processes, with *Cartwright's* [1978] model results. Also shown are the observations of 1PG emission from *Vallance Jones and Gattinger* [1976b, 1978] scaled with the 1PG transition probabilities of *Piper et al.* [1989]. Model results indicate the best fit occurs when all three collisional processes (quenching, ICT, and vibrational redistribution) are active, although the full measure of the observed enhancement of $v = 2$ is not achieved by the current model.

The relative populations of the $B\ ^3\Pi_g$ vibrational levels 3 through 9 at 130, 110, 95, and 80 km predicted by the current model is shown in Figure 9. Here all collisional processes are active. This figure shows that an enhancement of the higher vibrational levels is predicted at lower altitudes primarily due to the effect of collisional transfer (ICT) from the long-lived $N_2(A)$ and $N_2(W)$ states. Where such alterations occur, they give rise to an increase in the visually observed red emission from the 1PG. The effect is demonstrated in Figure 10 where the two spectra, that for 80 km and that for 130 km, have been scaled with the sensitivity function of the human eye [*Gebel*, 1964]. The total equilibrium population of the B state is the same for the two spectra shown here, but the solid spectrum, characterized by collisional rearrangement, embodies an enhancement in the total emission of visible red photons.

Figure 10 has been presented to emphasize the effect of the collisional redistribution of the emitted 1PG photons brought about by ICT. There is, however, the important additional consideration that most of the entire excitation of the B and the W is emitted as 1PG photons where ICT prevails. That is, when the W and B are collisionally coupled, 1PG transitions from the B to the A are far more probable than any optical transition from the W, and the 1PG constitutes the emission channel of choice for all of the W and B excitation. Since the W and B have roughly the same excitation rates in the aurora, the onset of ICT leads to a considerable augmentation of the overall 1PG intensity. Consequently, there is an enhancement of the 1PG over and above that produced by the combined effect of the redistributed B populations and the sensitivity of the human eye. This results

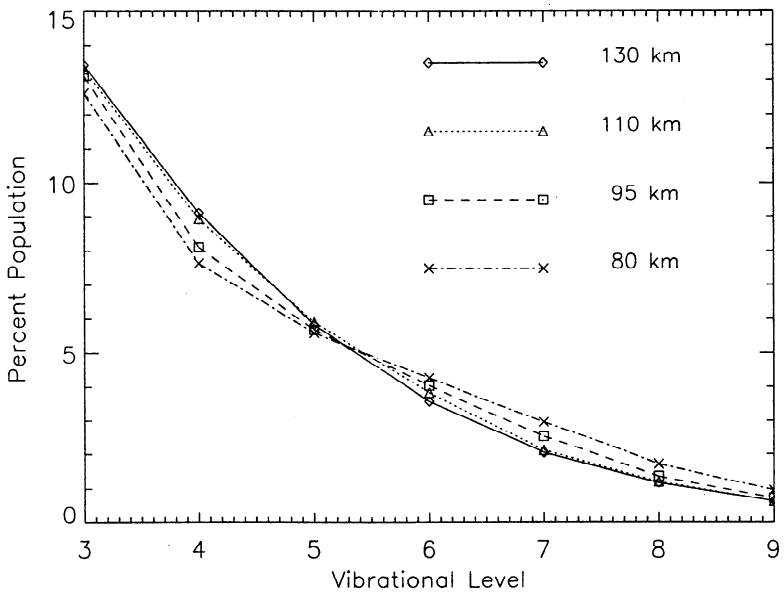

Figure 9. Percent population of the $B^3\Pi_g$ vibrational levels 3 through 9 at 130, 110, 95, and 80 km predicted by the current model with all collisional processes active. Note the enhancement in $v > 5$ for altitudes less than 90 km.

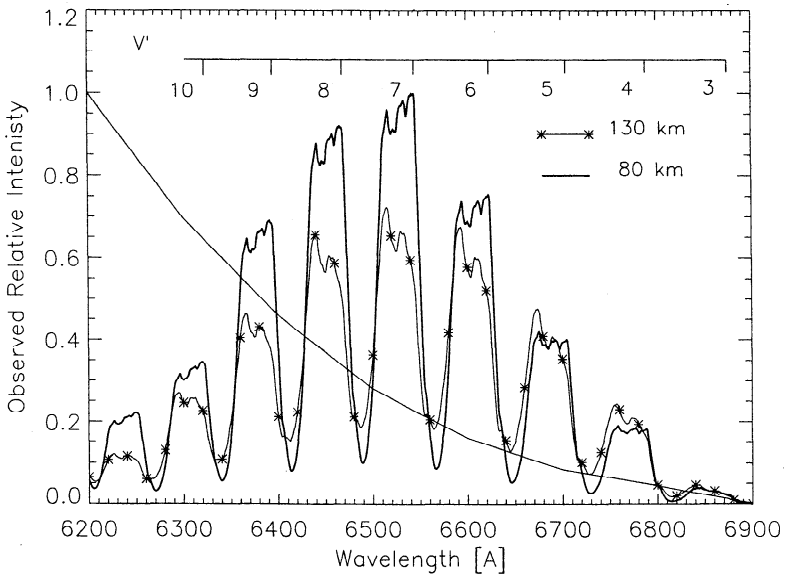

Figure 10. Model spectra of the 1PG $\Delta v = 3$ sequence predicted at 130 and 80 km produced by the distributions of Figure 9 and scaled with the sensitivity curve of the human eye. The resolution for these spectra is 9 Å. The total $B^3\Pi_g$ population for these two spectra is the same. This figure shows the predicted red enhancement to be observed visually as the aurora penetrates to lower altitudes (approximately 80 km).

in roughly a factor of 2 increase in the 1PG $\Delta v = 3$ volume emission rate due to ICT coupling primarily from the overlapping W state. Figure 11 shows the increase in the observed intensity due to both the enhancement in the B populations the sensitivity of the human eye [Gebel, 1964]. The populations of the B and W states at 80 km with and without ICT are shown in Figure 12. This figure shows the loss of W state population and corresponding gain in the B state population when ICT is included. As we have stated elsewhere [*Benesch*, 1981, 1983; *Morrill et al.*, 1988, 1991; *Morrill and Benesch*, 1990, 1994, 1995], we consider the effects of the ICT process to play a significant role in the variation of the $N_2(B)$ vibrational distribution and the production of the auroral red lower border.

4. Discussion

The considerations above address two distinct problems associated with auroral N_2 emission: the quenching of the $N_2(A)$ state, primarily by atomic oxygen, and the role of N_2 collisions in the variation of the $N_2(B)$ vibration populations.

Collisional deactivation of the $N_2(A)$ state has long been understood to be important [*Broadfoot and Hunten*, 1964; *Shemansky et al.*, 1971; *Sharp*, 1971] primarily because of its long radiative lifetime. Numerous values of the rate coefficients for the deactivation of $N_2(A)$ by O have been measured and compilations of these coefficients have appeared elsewhere [*Cartwright*, 1978; *Torr and Torr*, 1982; *Meier*, 1991] and

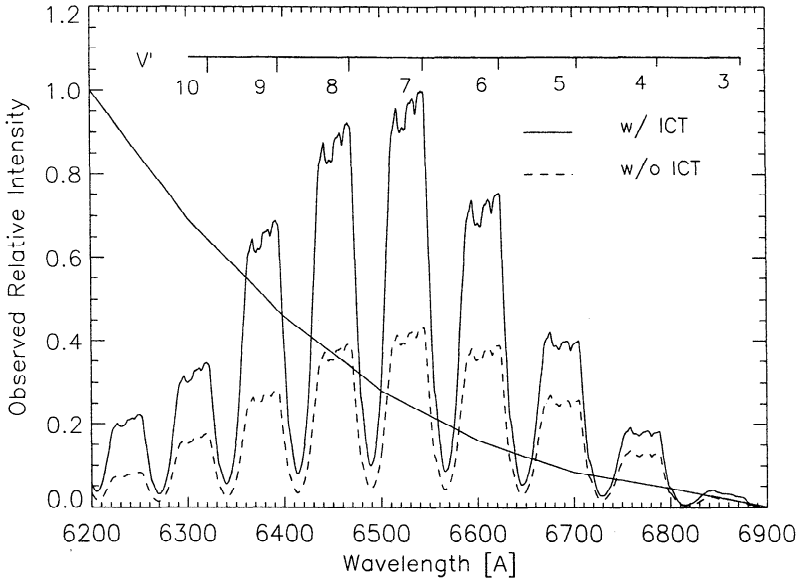

Figure 11. Comparison of $\Delta v = 3$ sequence predicted with and without ICT at 80 km. This figure includes the sensitivity of the eye (solid curve) and shows a significant enhancement (>2X) in the visible red intensity due to ICT.

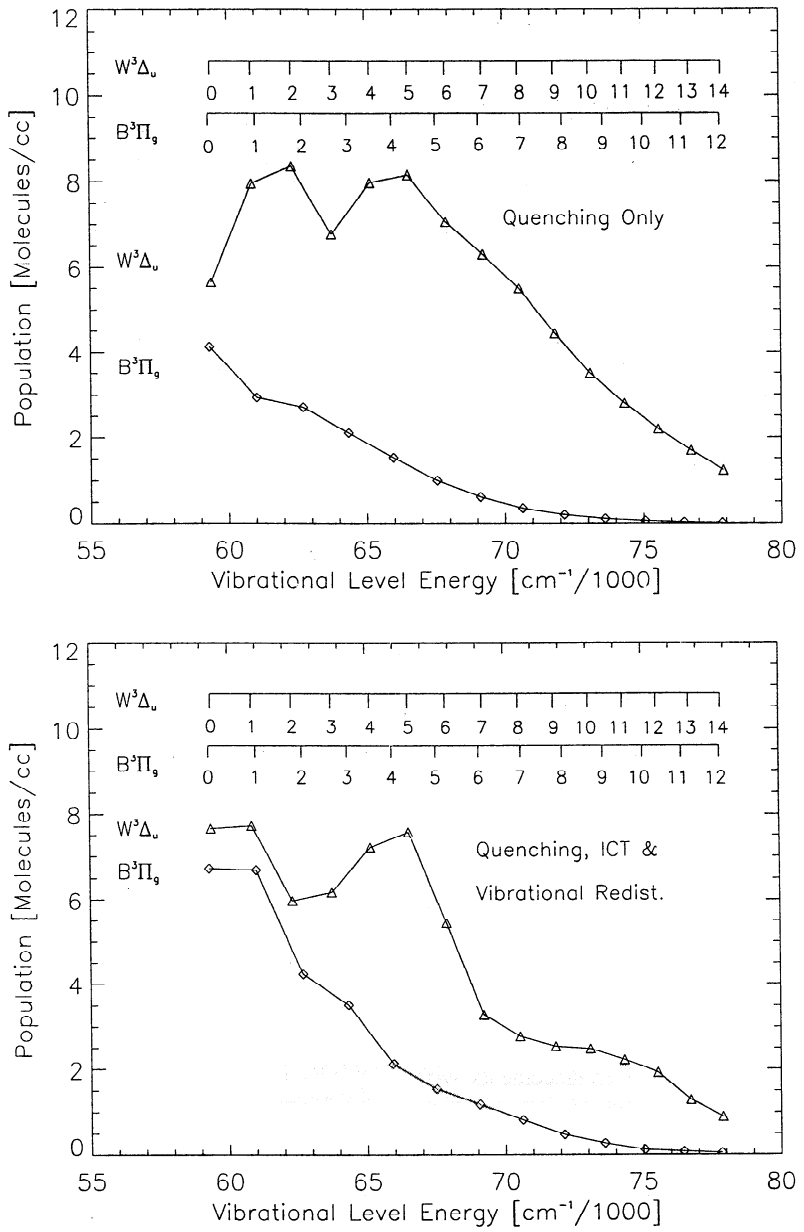

Figure 12. $B\,^3\Pi_g$ and $W\,^3\Delta_u$ vibrational distributions with and without ICT. The $W\,^3\Delta_u$ is a reservoir of population for the $B\,^3\Pi_g$ which can be accessed at lower altitudes with the increase in kinetic collisions. Note that for the case with ICT the $B\,^3\Pi_g$ and $W\,^3\Delta_u$ populations tend to draw together with increased resonance between vibrational levels.

range from $2x10^{-11}$ to $4x10^{-10}$ cm^3/molecule-second. The general tendency has been for the coefficients determined from atmospheric observations to be larger than the laboratory values by factors of 3 to 10. For the current study we have used the laboratory results of *Thomas and Kaufman* [1985] since their measurements cover the largest range of $N_2(A)$ vibrational levels. These results also include $N_2(A)$ quenching by O_2 which complement the earlier work by *Dreyer et al.* [1974] which was used by *Cartwright* [1978]. It is worth noting that Thomas and Kaufman's O-quenching coefficients are the largest of the recent values measured in the laboratory [*Piper et al.*, 1981; *Thomas and Kaufman*, 1985; *DeSouza et al.*, 1985] and this would contribute to our predicted column abundances of $N_2(A)$ being low compared to the observations of *Rees et al.* [1976] (see Figure 6). Given this comparison and the corroboration of the smaller rate coefficients by recent laboratory measurements, we consider the coefficients determined from atmospheric observations to be overestimates of the correct values.

The discrepancy between rate coefficients determined from atmospheric observations and those of laboratory studies is likely due to a number of factors. These include inaccuracies in the O density used in calculation, use of older $N_2(A)$ lifetimes rather than the more recent values which are approximately 25% larger [*Piper*, 1993], and possible additional loss mechanisms in the atmosphere [*Torr and Torr*, 1982]. Coefficients determined via laboratory techniques are insensitive to the radiative lifetime and the measurement of O densities can be done with relatively high accuracy [*Piper et al.*, 1981; *Thomas and Kaufman*, 1985]. Consequently, the use of the laboratory coefficients offers the possibility of measuring thermospheric O density profiles from

VK/2PG intensity ratios using techniques described elsewhere [*McDade and Llewellyn*, 1984]. We will present the results of this type of analysis in a future publication.

As to variations in the $N_2(B)$ vibrational distributions due to N_2 collisions, much of our previous work focuses on the corresponding spectral variations of the 1PG observed in laboratory N_2 discharges [*Benesch and Fraedrich*, 1984; *Morrill et al.*, 1988, 1991; *Morrill and Benesch*, 1990]. These variations are produced by changes in experimental conditions, specifically, pressure or the repetition rate of the excitation pulse. Such changes in conditions lead to alterations in the electron temperature during the excitation pulse which, in turn, produces corresponding changes in the relative excitation rate of the excited states under present discussion. By far, the most significant spectral variations occur as a result of changes in pressure [*Morrill et al.*, 1988] which reflects the molecular collision frequency. Of course, in the aurora, changes in altitude correspond to changes in collision frequency. For the long-lived N_2 triplet states, $A\,^3\Sigma_u^+$ and $W^3\Delta_u$, where the collision frequency exceeds the radiative lifetime, collisional transitions to the $B\,^3\Pi_g$ become more probable than emission. The $N_2(A)$ and $N_2(W)$ states represent a significant reservoir of excited state population which can be transferred to the $N_2(B)$ state with the increasing N_2 collision frequency which occurs at lower altitudes. This transfer of population results in enhancements in the 1PG band intensities, primarily for bands with $v' = 6 - 8$ (see ICT rate coefficients in Figure 3 and *Morrill et al.* [1988]). This is shown for the case of the $N_2(W)$ state in Figures 11 and 12.

As the results in Figure 9 show, collisional alterations in the $N_2(B)$ vibrational distribution are not predicted to occur until approximately 80-90 km. This shift produces an increase in the visually observable red emission from the 1PG $\Delta v = 3$ sequence as discussed above. It should be noted that significant changes in the $N_2(B,v>5)$ populations are not predicted for 95 km and above in agreement with auroral observations of the 1PG by *Gattinger et al.* [1985]. Given the correlation of the predicted altitude and spectral region of the 1PG enhancements with observations of natural and man-made deep red lower borders [*Stormer*, 1955; *Boquist and Synder*, 1967], we consider the N_2 1PG to be the probable source of this phenomenon. As noted by *Gattinger and Vallance Jones* [1979] there is historical evidence that red lower borders may occur at different heights with the ones near 100 km appearing "pink" and the ones near 80 km appearing "crimson." The present results apply specifically to the lower altitude "crimson" borders.

As early as 1938 Vegard observed the intense red lower border of type *b* aurora and remarked that they occur most frequently at sunspot minima [*Vegard*, 1938]. He presents spectra which show that enhancement of 1PG at the lower altitudes is a significant feature of type *b* red lower borders. One difficulty with verifying the spectral changes which our model calls for is that such features are often evanescent occurrences which move rapidly and unpredictability. Consequently, they are difficult to measure. However, a number of recent instruments [*Rairden and Swenson*, 1994, *Sivjee*, 1994] are beginning to make ground-based auroral measurements in the visible and near IR using CCD detectors. Such instruments collect time-resolved spectral images which contain altitude information. Thus they allow the repeated measurement of an entire spectrum of rapidly time-varying auroral forms which is a requirement for the capture of these elusive features.

5. Conclusions

Figures 5 through 12 display a number of results from the current model, some compared to observations. A comparison between the current model and *Cartwright's* [1978] model, using only cascade and quenching, shows that the results of the current model are in basic agreement with those of the earlier model, as shown in Figure 5. The current model also provides column abundances which fit well with simultaneous field observations of the $N_2(A)$, $N_2(B)$, and $N_2(C)$ states. It appears that improvements in the O and O_2 quenching coefficients and updated transition probabilities both play a major role in improving the fit between model $N_2(A)$ populations and observations (Figure 7c). In addition, vibrational redistribution provides a small but significant improvement in the prediction of $N_2(A)$ state vibrational populations primarily because it forces the population toward lower levels without the loss of $N_2(A)$ state molecules. Intersystem collisional transfer (ICT) strongly effects the vibrational level populations of the $N_2(B)$ state. Model results show both an improvement in the fit with observations for the low $N_2(B)$ state vibrational levels as well as an enhancement of the higher levels (v = 6-9) which is predicted to occur at lower altitudes (approximately 80-90 km). These latter changes in the $N_2(B)$ populations shift the center of the intensity distribution of the 1PG $\Delta v = 3$ sequence from the near infrared into the visible red. It should be noted that appreciable changes in the N_2 $(B,v>5)$ populations are not predicted until approximately 80-90 km, in agreement with 1PG observations at higher altitudes [Gattinger et al., 1985]. This behavior provides a probable explanation of the lower altitude deep-red lower border. Future plans for the model include the addition of the N_2 singlets and the estimation of thermospheric atomic oxygen density profiles using VK and 2PG band emission ratios.

Note added in proof. Recent interest in "Red Sprites", natural electric discharges appearing above the tops of thunderstorms, prompts us to call attention to the affinity of that phenomenon with the auroral red lower borders as discussed above. The spectrum of Red Sprites shows a dominant emission of molecular nitrogen 1PG, and the altitude domain of the Sprites impinges on that of the red lower border from below. Spectral observations of Sprites show an enhancement in the intensity of the bands in the $\Delta v = 3$ sequence of the 1PG over that observed in a normal aurora [Mende, et al., 1995; Hampton, et al., 1995]. This is consistent with the model outlined above which establishes that considerable intersystem collisional transfer of excitation occurs at pressures where Sprites are observed.

Acknowledgments. This material is based on work supported in part by the National Science Foundation under grant number ATM-8912154 and NASA grant NAGW 2168. The computer time was supported by the Upper Atmospheric Physics Branch and Solar Physics Branch, Space Science Division, Naval Research Laboratory. The authors would like to thank David Cartwright for his helpful and encouraging comments and for providing us with a copy of his N_2 excited state model, Eric Bucsela for his helpful and enjoyable conversations, and Susan Queen for her patience and critical review of the manuscript.

The editor thanks I. C. McDade and A. L. Broadfoot for their assistance in evaluating this paper.

References

Ajello, J. M., and D. E. Shemansky, A re-examination of important N_2 cross sections by electron impact with applications to the airglow: The Lyman-Birge-Hopfield band system, *J. Geophys. Res.*, *90*, 9845, 1985.

Alexander, M. H., and G. C. Corey, Collision induced transitions between $^2\Pi$ and $^2\Sigma$ states of diatomic molecules: Quantum theory and collisional propensity rules, *J. Chem. Phys.*, *84*, 100, 1986.

Alexander, M. H., and B. Pouilly, Symmetry selection rules in inelastic collisions of diatomic molecules in $^3\Pi$ electronic states , *J. Chem. Phys.*, *79*, 1545, 1983.

Ali, A., and P. L. Dagdigian, Rotational energy transfer within the $B^3\Pi_g$ $v = 3$ manifold of nitrogen, *J. Chem. Phys.*, *87*, 6915, 1987.

Bachmann, R., X. Li, C. Ottinger, and V. F. Vilesov, Molecular-beam study of the collisional intramolecular coupling of $N_2(B\,^3\Pi_g)$ with $N_2(A\,^3\Sigma_u^+)$ and $N_2(W\,^3\Delta_u)$ states, *J. Chem. Phys.*, *96*, 5151, 1992.

Bachmann, R., X. Li, C. Ottinger, V. F. Vilesov and V. Wulfmeyer, Vibrational-state-to- state collision-induced intramolecular energy transfer $N_2(A^3\Sigma_u^+ \rightarrow B^3\Pi_g)$, *J. Chem. Phys.*, *98*, 8608, 1993.

Benesch, W., Mechanism for the auroral red lower border, *J. Geophys. Res.*, *86*, 9065, 1981.

Benesch, W., Intersystem collisional transfer of excitation in low altitude aurora, *J. Chem. Phys.*, *78*, 2978, 1983.

Benesch, W., and D. Fraedrich, The role of intersystem collisional transfer of excitation in the determination of N_2 vibronic level populations. Applications to the $B\,'^3\Sigma_u^- \rightarrow B\,^3\Pi_g$ band intensity measurements, *J. Chem. Phys.*, *81*, 5367, 1984.

Benesch, W. M., and K. A. Saum, The $W^3\Delta_u$ state of molecular nitrogen, *J. Phys. B*:At. Mol. Opt. Phys., *4*, 732, 1971.

Boquist, W. P., and J. W. Snyder, Conjugate auroral measurements from the 1962 high altitude nuclear tests series, in *Aurora and Airglow Proceedings of the NATO Advanced Study Institute*, edited by Billy M. McCormac, pp 325, Reinhold, New York, 1967.

Brinkmann, R. T., and S. Trajmar, Electron impact excitation of N_2^*, *Ann. Geophys.*, *26*, 201, 1970.

Broadfoot, A. L., and D. M. Hunten, Excitation of N_2 band systems in Aurora, *Can. J. Phys.*, *42*, 1212, 1964.

Cartwright, D. C., Total cross sections for the excitation of the triplet states in molecular nitrogen, *Phys. Rev. A*, *2*, 1331, 1970.

Cartwright, D. C., Vibrational Populations of the excited states of N_2 under auroral conditions, *J. Geophys. Res.*, *83*, 517, 1978.

Cartwright, D. C., S. Trajmar, and W. Williams, Vibrational populations of the $A^3\Sigma_u^+$ and $B\,^3\Pi_g$ states of N_2 on normal auroras, *J. Geophys. Res.*, *76*, 8368, 1971.

Cartwright, D. C., S. Trajmar, and W. Williams, Reply, *J. Geophys. Res.*, *78*, 2365, 1973.

Cartwright, D. C., A. Chutjian, S. Trajmar, and W. Williams, Electron impact excitation of the electronic states of N_2, I, Differential cross sections at incident energies from 10 to 50 eV, *Phys. Rev. A*, *16*, 1013, 1977a.

Cartwright, D. C., A. Chutjian, S. Trajmar, and W. Williams, Electron impact excitation of the electronic states of N_2, II, Integral cross sections at incident energies from 10 to 50 eV, *Phys. Rev. A*, *16*, 1041, 1977b.

Chutjian, A., D. C. Cartwright, and S. Trajmar, Electron impact excitation of the electronic states of N_2, III, Transitions in the 12.5-14.2 eV energy-loss region at incident energies of 40 and 60 eV, *Phys. Rev. A*, *16*, 1052, 1977.

DeSouza, A. R., G. Gousset, M. Touzeau, and T. Khiet, Note of the determination of the efficiency of the reaction $N_2(A^3\Sigma_u^+) + O(^3P) \rightarrow N_2 + O(^1S)$, *J. Phys. B At. Mol. Phys.*, *18*, L661, 1985.

Dreyer, J. W., and D. Perner, Deactivation of $N_2(B\,^3\Pi_g, v = 0\text{-}7)$ and $N_2(a'^1\Sigma_u^-, v = 0)$ by nitrogen, *Chem. Phys. Lett.*, *16*, 169, 1972.

Dreyer, J. W., and D. Perner, Deactivation of $N_2(A^3\Sigma_u^+, v = 0\text{-}7)$ by ground state nitrogen, ethane, and ethylene measured by kinetic absorption spectroscopy, *J. Chem. Phys.*, *58*, 1195, 1973.

Dreyer J. W., D. Perner, and C. R. Roy, Rate constants for the quenching of $N_2(A^3\Sigma_u^+, v = 0\text{-}8)$ by CO, CO_2, NH_3, NO, and O_2, *J. Chem. Phys.*, *61*, 3164, 1974.

Eastes, R. W., and W. E. Sharp, Rocket-borne spectroscopic measurements in the ultraviolet aurora: The Lyman-Birge-Hopfield Bands, *J. Geophys. Res.*, *92*, 10095, 1987.

Eastes, R. W., A. V. Dentamaro, and D. T. Decker, Collision induced transitions between the $a'^1\Sigma_u^-$, $w^1\Delta_u$, and $a^1\Pi_g$ states of N_2: How they effect N_2 Lyman-Birge-Hopfield band emission from the earth's airglow and aurora (abstract), Eos Trans. *AGU, 75*(16), Spring Meet. Suppl., 251, 1994.

Espy, P. J., A spectroscopic investigation of the infrared molecular band systems of N_2 and N_2^+ resulting from low energy electron impact excitation, Ph.D. dissertation, Utah State Univ., Logan, 1986.

Feldman, P. D., and J. P. Doering, Auroral electrons and the optical emission of nitrogen, *J. Geophys. Res.*, *80*, 2808, 1975.

Gattinger, R. L. and A. Vallance Jones, Observations and interpretations of spectra and rapid time-variations of type-b aurora, *Planet. Space Sci.*, *27* 169, 1979.

Gattinger, R. L., F. R. Harris, and A. Vallance Jones, The height, spectrum and mechanism of type-b red aurora and its bearing on the excitation of O (^{1}S) in aurora, *Planet. Space Sci.*, *33*, 207, 1985.

Gebel, R. K. H., *The Threshold of Visual Sensation of Comparison With That of Photodetectors, Its Quantum Aspect, Problems of Color Perception, and Related Subjects*, Aerosp. Res. Lab., Office of Aerosp. Res., U.S. Govt. Print. Off., Washington, D. C., 1964.

Gilmore, F. R., Comment, *Can. J. Chem.*, *47*, 1779, 1969.

Gilmore, F. R., R. R. Laher, and P. J. Espy, Franck-Condon factors, r-centroids, electronic transition moments, and Einstein coefficients for many nitrogen and oxygen systems, *J. Phys. Chem. Ref. Data, 21*, 1005, 1992.

Hampton, D. L., M. J. Heavner, E. M. Wescott, and D. D. Sentman, Optical spectral characteristics of sprites, *Geophys. Res. Lett., in press*, 1995.

Heidner, R. F., III, D. G. Sutton, and S. N. Suchard, Kinetic study of N_2 ($B\,^3\Pi_g$,v) quenching by laser induced fluorescence, *Chem. Phys. Lett.*, *37*, 243, 1976.

Jursa A. S., (Ed.), *Handbook of Geophysics and the Space Environment*, Air Force Geophys. Lab., U. S. Govt. Print. Off., Washington, D. C., 1985.

Katayama, D. H., Collision induced electronic energy transfer between the $A^2\Pi_{ui}(v = 4)$ and $X^1\Sigma_g^+(v = 8)$ rotational manifolds of N_2^+, *J. Chem. Phys.*, *81*, 3495, 1984.

Katayama, D. H., and A. V. Dentamaro, Propensities for collision induced electronic transitions in a diatomic molecule, *J. Chem. Phys.*, *85*, 2595, 1986.

Katayama, D. H., and A. V. Dentamaro, Electronic transitions from the $A^2\Pi_{ui}(v=3)$ level of N_2^+ induced by inelastic collisions with helium atoms, *J. Chem. Phys.*, *91*, 4571, 1989.

Marinelli, W. J., W. J. Kessler, B. D. Green, and W. A. M. Blumberg, Quenching of $N_2(a^1\Pi_g, v = 0)$ by N_2, O_2, CO, CO_2, H_2, and Ar. *J. Chem. Phys.*, *90*, 2167, 1989.

McConkey, J. W., and F. R. Simpson, Electron impact excitation of the $B\,^3\Pi_g$ state of N_2, *J Phys. B At. Mol. Opt. Phys.*, *2*, 923, 1969.

McDade, I. C., and E. S. Llewellyn, Atomic oxygen concentration in the auroral ionosphere, *Geophys. Res. Lett.*, *11*, 247 1984.

Meier, R. R., Ultraviolet spectroscopy and remote sensing of the upper atmosphere, *Space Sci. Rev.*, *58*, 1, 1991.

Mende, S. B., R. L. Rairden, and G. R. Swenson, Sprite Spectra; N_2 1PG band identification, *Geophys. Res. Lett.*, *22*, 2633, 1995.

Morrill, J., and W. Benesch, Plasma preconditioning and the role of elevated vibrational temperature in production of excited N_2 vibrational distributions, *J. Geophys. Res.*, *95*, 7711, 1990.

Morrill, J. S., and W. M. Benesch, The effect of collisional processes on N_2 triplet vibrational populations under auroral conditions; Preliminary model results (abstract), Eos Trans. *AGU, 75* (16) Spring Meet. Suppl., 252, 1994.

Morrill, J. S., and W. M. Benesch, Auroral N_2 triplet emissions: Vibrational populations and the effect of collisional processes, *U. S. Nat. Rep. Int. Union Geod. Geophys. 1991-1994, Rev. Geophys., 33*, B70, 1995.

Morrill, J., B. A. Carragher, and W. Benesch, Population development of auroral molecular nitrogen species in a pulsed discharge, *J. Geophys. Res.*, *93*, 963, 1988.

Morrill, J. S., W. M. Benesch, and K. G. Widing, Electron temperatures in a pulse electric discharge and the associated N_2 electron excitation rate coefficients, *J. Chem. Phys.*, *94*, 262, 1991.

Piper, L. G., Quenching rate coefficients for $N_2(a\,'\,^1\Sigma_u^-)$, *J. Chem. Phys.*, *87*, 1625, 1987.

Piper, L. G., State-to-state $N_2(A^3\Sigma_u^+)$ energy pooling reactions, II, The formation and quenching of $N_2(B\,^3\Pi_g, v = 1\text{-}12)$, *J. Chem. Phys.*, *88*, 6911, 1988.

Piper, L. G., Reevaluation of the transition-moment function and Einstein coefficients for the $N_2(A^3\Sigma_u^+\text{-}X^1\Sigma_g)$ transition, *J. Chem. Phys.*, *99*, 3174, 1993.

Piper, L. G., G. E. Caledonia, and J. P. Kennealy, Rate coefficients for deactivation of $N_2(A^3\Sigma_u^+, v = 0,1)$ by O, *J. Chem. Phys.*, *75*, 2847, 1981.

Piper, L. G., K. W. Holtzclaw, and B. D. Green, Experimental determination of the Einstein coefficients for the $N_2(B\text{-}A)$ transition, *J. Chem. Phys.*, *90*, 5337, 1989.

Rairden, R., and G. Swenson, New imaging spectrometer for auroral research, *Proc. SPIE Int. Soc. Opt. Eng.*,, *2266*, 221, 1994.

Rees, M. H., and K. Maeda, Auroral electron spectra, *J. Geophys. Res.*, *78*, 8391, 1973.

Rees, M. H., G. G. Sivjee, and K. A. Dick, Studies of molecular nitrogen bands from airborne auroral spectroscopy, *J. Geophys. Res.*, *81*, 6046, 1976.

Rotem, A., and S. Rosenwaks, Laser-induced fluorescence studies of molecular nitrogen, *Opt. Eng.*, *22*, 564, 1983.

Rotem, A., I. Nadler, and S. Rosenwaks, Direct observation of collision induced transitions from $N_2(B\,^3\Pi_g)$ to $N_2(B\,'\,^3\Sigma_u^-)$, *J. Chem. Phys.*, *76*, 2109, 1982.

Sadeghi, N., and D. W. Setser, Collisional coupling of $N_2(B^3\Pi_g)$ and $N_2(W^3\Delta_u)$ states studied by laser-induced fluorescence, *Chem. Phys. Lett.*, *77*, 304, 1981.

Sharp, W. E., Rocket-borne spectroscopic measurements in the ultraviolet aurora: Nitrogen Vegard-Kaplan bands, *J. Geophys. Res.*, *76*, 987, 1971.

Shemansky, D. E., and A. L. Broadfoot, Excitation of N_2 and N_2^+ systems by electrons, 2, Excitation cross-sections and N_2 1PG low pressure afterglow, *J. Quant. Spectros. Radiat. Transfer*, *11*, 1401, 1971.

Shemansky, D. E., and A. L. Broadfoot, Comment on paper by D. C. Cartwright, S. Trajmar, and W. Williams, "Vibrational populations of the $A^3\Sigma_u^+$ and $B\,^3\Pi_g$ states of N_2 in normal auroras," *J. Geophys. Res.*, *78*, 2357, 1973.

Shemansky, D. E., and A. Vallance Jones, Type-b red aurora; The O_2^+ first negative system and the N_2 first positive system, *Planet. Space Sci.*, 1115, 1968.

Shemansky, D. E., E. C. Zipf, and T. M. Donahue, Deactivation of $N_2A^3\Sigma_u^+$ molecules in the aurora, *Planet. Space Sci.*, 19, 1669, 1971.

Sivjee, G. G., Spectroscopy and imagery of airglow and aurora (abstract), Eos Trans. *AGU, 74* (16), Spring Meet. Suppl., 248, 1994.

Solomon, S. C., Auroral excitation of the N_2 2P(0,0) and VK(0,9) bands, *J. Geophys. Res.*, *94*, 17,215, 1989.

Stanton, P. N., and R. M. St. John, Electron Excitation of the first positive bands of N_2 and of the first negative and Meinel bands of N_2^+, *J. Opt. Soc. Am.*, *59*, 252, 1969.

Stormer, C., *The Polar Aurora*, Clarendon, Oxford, 1955.

Strickland, D., R. E. Daniell, Jr., J. R. Jasperse, and B. Basu, Transport-theoretic model for the electron-proton-hydrogen atom aurora, 2, Model results, *J. Geophys. Res.*, *98*, 21,533, 1993.

Thomas, J. M., and F. Kaufman, Rate constants of the reactions of metastable $N_2(A^3\Sigma_u^+)$ in $v = 0,1,2$, and 3 with ground state O_2 and O, *J. Chem. Phys.*, *83*, 290, 1985.

Torr, M. R., and D. G. Torr, The role of metastable species in the thermosphere, *Rev. Geophys. Space Phys.*, *20*, 91, 1982.

Trajmar, S., D. F. Register, and A. Chutjian, Electron scattering by molecules, II, Experimental methods and data, *Phys. Rep.*, *97*, 219, 1983.

Vallance Jones, A., *Aurora Geophysics and Astrophysics Monographs*, D. Reidel, Hingham, Mass., 1974.

Vallance Jones, A., and R. L. Gattinger, Quenching of the N_2 Vegard-Kaplan system in the aurora, *J. Geophys. Res.*, *81*, 497, 1976a.

Vallance Jones, A., and R. L. Gattinger, Quantitative spectroscopy of the aurora, IV, The spectrum of medium intensity aurora between 8800Å and 11400Å, *Can. J. Phys.*, *54*, 2128, 1976b.

Vallance Jones, A., and R. L. Gattinger, Vibrational development and quenching effects in the $N_2(B^3\Pi_g\text{-}A^3\Sigma_u^+)$ and $N_2^+(A^2\Pi_u\text{-}X^2\Sigma_g^+)$ system in aurora, *J. Geophys. Res.*, *83*, 3255, 1978.

Vegard, L., Altitude effects in the red part of the auroral spectrum and the two types of red auroras, *Nature*, *141*, 200, 1938.

Wu, H. L., and W. Benesch, Evidence for the $^3\Delta_u \rightarrow B^3\Pi_g$ transition in N_2, *Phys. Rev.*, *172*, 31, 1968.

Zubek, M., Excitation of the $C\,^3\Pi_u$ state of N_2 by electron impact in the near-threshold region, *J. Phys. B At. Mol. Opt. Phys.*, *27*, 573, 1994.

Zubek, M., and G. C. King, Differential cross sections for electron impact excitation of the $C\,^3\Pi_u$, $E\,^3\Sigma_g^+$, and $a'\,^1\Sigma_g^+$ states of N_2, *J. Phys B At. Mol. Opt. Phys.*, *27*, 2613, 1994.

W. M. Benesch, Institute for Physical Science and Technology, University of Maryland, College Park Maryland, 20742

J. S. Morrill, E. O. Hulburt Center for Space Research, Naval Research Laboratory, 4555 Overlook Ave., Code 7660, Washington, DC 20375-5320. (e-mail: morrill@louis14.nrl.navy.mil)

(Received March 6, 1995; revised August 21, 1995; accepted September 11, 1995.)